Overview of the Kansas Windfarm2013 Field Program

Kenneth L. Cummins and Mason G. Quick[1]; William Rison, Paul Krehbiel, Ron Thomas, and Dan Rodeheffer[2];
Tom A. Warner[3]; Marcelo M.F. Saba and Carina Schumann[4]; Jackson Myers[5], Walter Lyons[6];
Amitabh Nag, John Cramer and Tommy Turner[7]; Tim Samaras, Paul Samaras and Carl Young[8];
Geoff Mcharg and Joshua Engle[9]; Steven A. Cummer and Gaopeng Lu[10]

1. University of Arizona, Tucson, Arizona, USA, 2. New Mexico Tech, Socorro, New Mexico, USA,
3. ZT Research, Rapid City, South Dakota, USA, 4. INPE, Brazil, 5. EDPR, Houston, Texas, USA,
6. FMA Research Inc., Fort Collins, Colorado, USA, 7. Vaisala, Tucson, Arizona, USA,
8. Samaras Technologies, Bennett, Colorado, USA, 9. U.S. Air Force Academy, Colorado Springs,
Colorado, USA, 10. Duke University, Durham, North Carolina, USA

ABSTRACT: Initial observations of lightning attachment to wind turbine generators at a Kansas wind farm in 2012 resulted in a number of insights and left several open questions. This led to the planning and re-deployment for the summer or 2013. Ten groups have collaborated on this 2013 field project, resulting in the following suite of instruments and observations: 10-station 3D lightning mapping array (LMA), 8-station slow antenna array, 4 electric field mills, 2 continuous, standard-speed, fixed-location video cameras, three mobile high-speed video observation vehicles, remote charge-moment observations, remote low-light cameras focusing on upper-atmospheric discharges, and upgraded U.S. National Lightning Detection Network observations of both cloud and cloud-to-ground discharges (including continuous waveform data). In addition, all turbine generators are equipped with devices that provide estimates of lightning peak current within the blades. This presentation will provide an overview of the 2012 and 2013 observations, including a brief discussion of the instruments, seasonal overviews of lighting incidence by type, turbine attachment statistics, and an example of downward attachment to wind turbines.

INTRODUCTION

Lightning attachment to tall objects has been studied for decades. The attachment of lightning to electric power transmission towers in elevated terrain has driven much of the quantitative assessment of lightning characteristics in the 1970's and 80's. This has led to the understanding that in flat terrain, the probability of upward-initiated lightning is negligible for tower heights less than 100 m. For tower heights greater than 100 m, the probability increases roughly linearly with the log of height, reaching 100% at a height of about 400 m. Additionally, the probability of upward initiation increases when the object resides on locally-elevated terrain. Recently, there has been renewed interest in the study of lightning attachment to tall objects in general, and wind turbines in particular, following the construction of large wind farms in lightning-prone regions (Warner et al. 2012; Montanyà et al. 2013, and others) .

Initial observations of lightning attachment to wind turbine generators at a Kansas wind farm in 2012 by some of the authors resulted in a number of insights and left several open questions (Wilson et al., 2013). This led to the planning and re-deployment for the summer of 2013. Ten groups have collaborated on this 2013 field program, resulting in the following suite of instruments and observations: 10-station 3D

lightning mapping array (LMA), 8-station slow E-field antenna array, 2 electric field mills, 2 continuous, standard-speed, fixed-location video cameras, three mobile high-speed video observation vehicles, remote charge-moment observations, remote low-light cameras focusing on upper-atmospheric discharges, and the upgraded U.S. National Lightning Detection Network observations of both cloud and cloud-to-ground discharges (including continuous waveform data). In addition, all turbine generators were equipped with devices that provide estimates of lightning currents within the blades.

This paper provides an overview of the 2012 and 2013 observations, including a brief discussion of the instruments, seasonal overviews of lighting incidence by type, turbine attachment statistics, and an example of downward attachment to wind turbines..

2012 CAMPAIGN SUMMARY

Wind Farm Topology

The terrain variations within the Kansas wind farm are characterized by small rolling hills with peak variations on the order of 25 m. The 60+ turbines are organized into west and east groups, divided by an Operations and Maintenance (O&M) building. All turbines have a hub height of 80 m, and blade lengths of 45 m, reaching a maximum height of 125 m. The typical distance between turbines at this wind farm is in the range of 350-800m.

Regional Lightning Climatology

Both the 2012 and 2013 campaigns took place during the convective season (May-September) in and near the wind farm, located in the U.S. central Great Plains. Storms in this region include small isolated thunderstorms, synoptically-driven mesoscale convective systems, and multicellular complexes that can include convective cells whose CG flash populations are positive-polarity-dominated and/or negative-dominated (Carey et al., 2003; Fleenor et al., 2009). This region is at the edge of the area within the U.S. with the highest incidence of severe weather, including large hail and tornados (Carey and Rutledge, 2003).
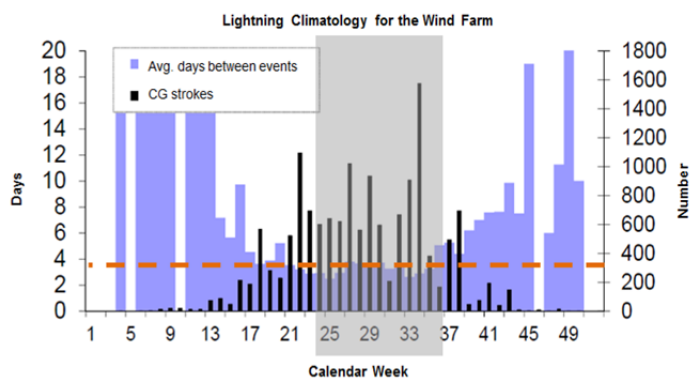

Fig. 1.   Eleven-year lightning climatology for a 20 km radius around the center of the wind farm (O&M building). The gray shaded weeks represent the period of the field studies (weeks 24-36). The orange dashed line shows the average CG strokes (363) per week during the 2012 campaign, far below the climate averages.

The mean weekly lightning incidence within 20 km of the wind farm is shown in Figure 1.   The blue histogram shows an 11-year average number of days between storms for each calendar week, starting in 2000. This varies between three (3) and four (4) days for our study period (gray rectangle). The black histogram shows the weekly average number of CG strokes for this region. This number is quite variable, ranging from 200 to 1,000 strokes per week, with a typical value near 600. For the 2012 field study, the

average weekly number of CG strokes within 20 km of the center of the wind farm was 363, which is well below average for this area. The average number of days between lightning-producing storms during the 2012 campaign was 3.73, which is typical.

Observation Systems

Observations for the 2012 campaign included standard-speed video observations from two cameras, static electric field using two electric field mills, NLDN observations of cloud-to-ground (CG) return strokes, and in-situ current transient measurements in all turbine blades reported by the "Supervisory Control and Data Acquisition" (SCADA) system. The two digital video camera systems (60 fields-per-second) were configured to self-trigger 2-second video sequences using a sequential-field-subtraction scene analysis (ufo-Capture). The two cameras had a small common field of view that included 8 of the wind turbines. Nearby NLDN sensors were configured to record information that allows reconstruction of magnetic field waveforms within the bandwidth of the NLDN sensors. The on-site instrumentation is shown in Figure 2.

Summary of Findings

During the 2012 field campaign seven (7) lightning strikes to wind turbines were captured by the video cameras with two (2) causing damage. Blade damage was also caused by an eighth lightning strike that was off-camera but detected by the NLDN. All observed wind turbine lightning attachments were to the blades. Analysis of the CG lightning data indicates that wind turbines with rotating blade tip heights of ~120 m have a larger attractive radius (276 m) than is expected for stationary towers of similar height, and an equivalent attractive radius to a nearby 231 m radio tower. There was no clear correlation between NLDN peak currents, SCADA-derived blade currents, and blade damage. It was clear from this study that the SCADA-derived current magnitudes did not represent the peak currents within the blades. More details are provided in Wilson et al, 2013.

Fig. 2.   (From left to right) Video camera installation at the Operations & Maintenance Building; video camera installation at the sub-station; map of the video camera viewing angles; view of an electric field mill installed at the wind farm.

There were only four known cases of upward initiated lighting within the wind farm during the 2012 campaign. One of these cases resulted in blade damage, and all of them occurred within the trailing stratiform region of large multi-cellular storms. The NLDN reported the nearby high-current discharges that triggered the upward leaders, but did not report current transients in the turbine blades unless they were associated with return-stroke like processes.

The NLDN also reported at least one CG stroke for each 24 SCADA-reported turbine strikes that were associated with downward flashes. Details about the accuracy of these NLDN reports are presented Cummins et al. 2014

At the conclusion of the analysis of the 2012 campaign, we were left with (1) uncertainty about the specific storm-electrical conditions that resulted in upward lightning discharges; (2) no real insight into the characteristics of the lightning that resulted in blade damage; and (3) an insufficient number of upward and damage-causing cases to make confident inferences about the likelihood of damage due to upward discharges with no fast current processes. Additionally, the NLDN was to undergo a significant upgrade during the spring of 2013, in order to improve the detection of cloud lightning flashes. Given these open issues, a plan was developed to carry out a much larger and more-complete field campaign in 2013, discussed below.

2013 CAMPAIGN

The 2013 campaign started in early May with the installation of the 10-station Lightning Mapping Array (LMA), and continued until September 3 when the LMA was removed.   Various instruments and projects teams made measurements during portions of the time period, as discussed in later sections. Subsequent subsections include an overview of thunderstorm activity, a description of a unique inverted-polarity storm case, a summary of turbine interactions, and selected examples of simultaneous instrument observations.

Observation Systems and Teams

Ten groups have collaborated on this 2013 field program, resulting in the following suite of instruments and observations:
- 10-station 3D lightning mapping array (LMA)
- 8-station slow antenna network
- 2 electric field mills
- 2 continuous, standard-speed, fixed-location video cameras,
- 3 mobile high-speed video observation vehicles
- remote charge-moment observations provided by the National Charge Moment Change Network
- remote low-light cameras focusing on upper-atmospheric discharges
- U.S. National Lightning Detection Network observations
- In-situ lightning current transient measurements for all turbine blades

A graphical overview of both the instrumentation and the observation locations is shown in Fig. 3. The LMA network provided VHF-based 3-dimensional mapping of both cloud and cloud-to-ground flashes, resulting from mapping the processes associated with electrical breakdown (Rison et al. 2000, Krehbiel et

al 2000, Thomas et al., 2004). The LMA stations were the current "portable LMA" configuration composed of the basic LMA station with local data storage, solar power, and cellular data radio modems. The communications bandwidth (200 kbps) was sufficient to provide both a command-and-control interface and 400 µS "decimated" data transfer for real-time lightning monitoring. Full-resolution data from the LMA sensors were downloaded at later times, as needed. Fig. 4 shows one of the LMA sties. The 10 LMA stations were separated by about 7-10 km, as shown in Fig. 3 (red asterisks).
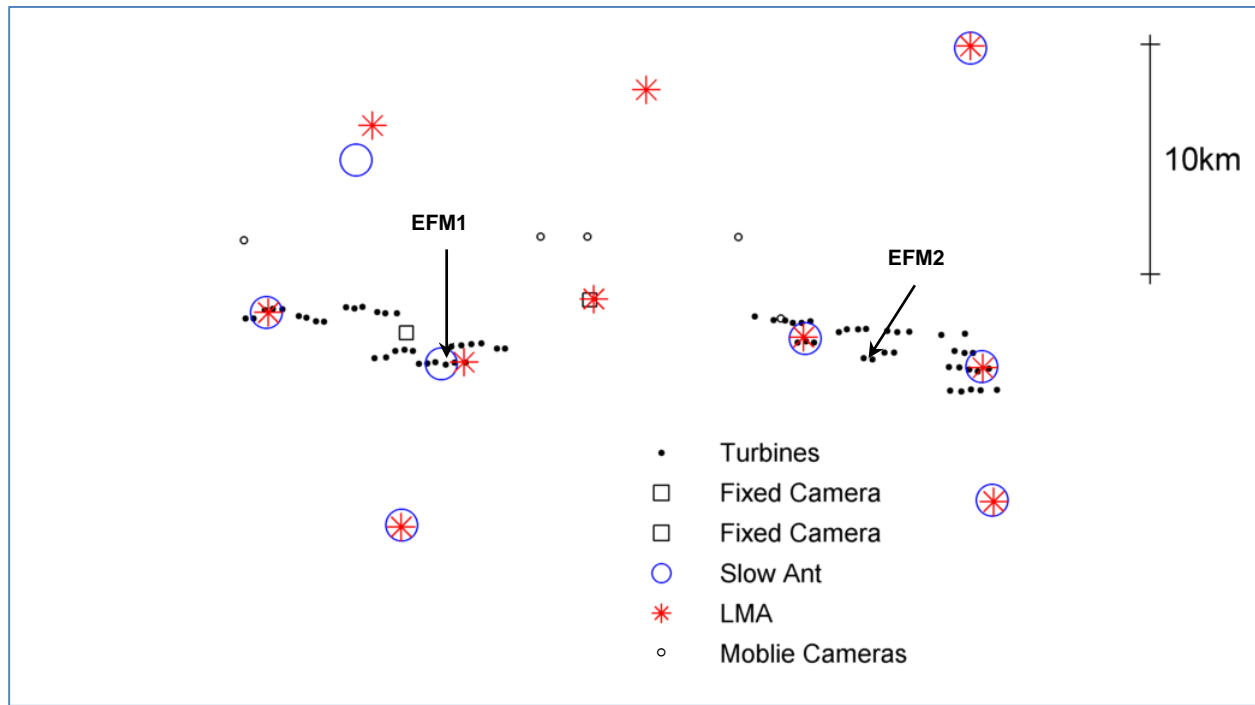
Fig. 3.   Overview of the 2013 campaign instrumentation. See text for details.

The LMA flash detection efficiency for this short baseline configuration is expected to be close to 100% within 150 km of the center of the wind farm. The number of LMA sources per flash will uniformly fall off for radial distances beyond a perimeter defined by the locations of the "outer" LMA sensors in the network. The modeled 2-dimensional radial location accuracy is shown in Fig 5a. The assumed 25 ns RMS timing error for this short baseline configuration yields less than 40 m radial errors within ~25 km of the center of the wind farm, and stays below 1 km out to a range of 100 km. The expected altitude accuracy above the freezing level remains below 100 m RMS out to 50 km, as shown in Fig. 5c.

Fig. 4. Portable Lightning Mapping Array (LMA) Station.

Since some of our work at the wind farm involves understanding electrical breakdown at wind turbine hub heights, the expected location accuracy at ~80m AGL (~500m MSL) was also evaluated. These results are shown in Fig. 5b. The expected RMS hub-height altitude error above the LMA sensors is less than 50 m, and remains less than 200 throughout most of the wind farm.
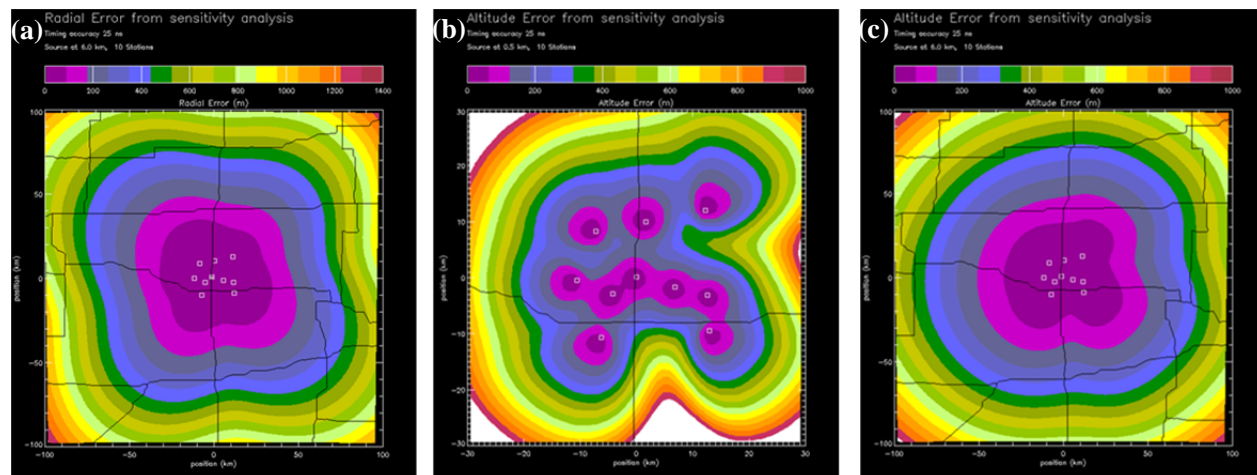

Fig. 5. Estimated Location Accuracy for the KSLMA.(left) RMS Radial error; (right) altitude error above the freezing level; (center) altitude error near turbine hub height.

The 8-station slow antenna network provided information about the times, locations, polarity, and magnitudes of lightning processes associated with significant charge transfer. The slow antenna sensors, designed by New Mexico Tech, had a low-frequency time constant of 10 seconds, and an upper frequency response of 25 kHz. The data were sampled at a 50 kHz rate. The nominal sensitivity of the sensors allowed them to accurately measure field changes in the range of 10 mV/m to 10 kV/m. Fig. 6 shows one of these slow antennas as installed in Kansas.

The electric field mills (EFMs) and standard-speed automatic cameras were the same ones that were used in 2012, as shown in Fig. 2. The EFM locations where changed in 2013, indicated by arrows in Fig. 3. The NLDN observations included both cloud and cloud-to-ground discharges, as well as continuous waveform data. In addition, all turbine generators were equipped with devices that provide estimates of lightning peak current within the blades, as was the case in 2012.

Fig. 6. New Mexico Tech solar-powered slow antenna installation. Battery box is being installed by Ron Thomas and Mason Quick, while being well-managed by our illustrious Brazilian team.

The mobile high-speed video observation vehicles were operated by three different groups. ZT Research, in collaboration with scientists from INPE (Brazil) and the University of Arizona (USA), operated 2 high-speed cameras: a Phantom v310 (typically at 11k or 35k fps) and a Miro 4 (typically at 1000 fps). Their period of observation was May 21 through June 8, 2013. FMA Research operated the Lightning Investigation Vehicle (LIV) in the area through 31 May 2013. It was equipped with a turret-mounted Phantom v7.3 high speed imager. The Phantom captured 6 CGs in the area of the wind farm, plus a lightning triggered upward lightning (LTUL) event resulting from the passage overhead of an intra-cloud leader on 29 May 2013 (Lyons et al., 2014). Researchers from the U.S. Air Force Academy operated a Phantom 7v7.1 camera and a low-light Watec camera from June 8 through July 3.

FMA Research and Duke University also maintained surveillance of the middle atmosphere above the wind farm using SpriteNet Watec 902H U cameras located at Yucca Ridge and Bennett, CO and Lubbock, TX. A sprite was captured coincident with LTUL event from a sprite-parent +CG on 30 May 2013 (Lyons et al., 2014).

Thunderstorm Occurrence Overview

For the 2013 field campaign, the average weekly number of CG strokes within 20 km of the center of the wind farm was 432. This is somewhat below average but is about 20% higher than for the 2012 campaign. The average number of days between lightning-producing storms in 2013 was 3.18, which is typical and higher than for 2012.

Time-series plots of lightning information reported by the NLDN within 80 km of the O&M building are shown in Fig. 7.   Fig. 7a provides an overview of the lightning for May 1 through early November 2103. The vertical bars represent 10-minute counts for negative CG stroke (green) and positive CG strokes (blue). The magenta dashed lines show the IC:CG ratio for individual 10-minute periods. This is the count of CG strokes for each 10-minute period, divided by its associated count of cloud pulses. Note that this is NOT the IC:CG flash ratio, but is will be highly correlated with it. The NLDN was upgraded for improved cloud-pulse detection on this area during the first week of May. This improvement can be seen in the "jump" in IC:CG ratio starting with the third storm in May (shown more clearly in Fig 7b). Quantitative assessment of this improvement is provided in conference papers by Cummins et al. (2014) and Murphy and Nag (2014).

Fig. 7b provides a zoom-in of this figure for the first three weeks of May. Severe storm report periods within 80 km of the O&M building are indicated red bars. Of particular interest is the storm that started near 00z on May 19. Note that there are an extremely high percentage of positive strokes. This particular storm was a very large squall line that developed a few hours earlier, becoming a highly organized severe storm when it reached the wind farm at about 03z. The National Mosaic & Multi-sensor QPE (NMQ) mosaic composite reflectivity for this storm at 03z is shown in Fig. 8, showing that this squall line was continuous across Nebraska and Kansas, and had two bowed segments. Between 03:10 and 03:50 there were SPC reports of tornados, hail, and high winds (>50 mph) in surrounding areas.
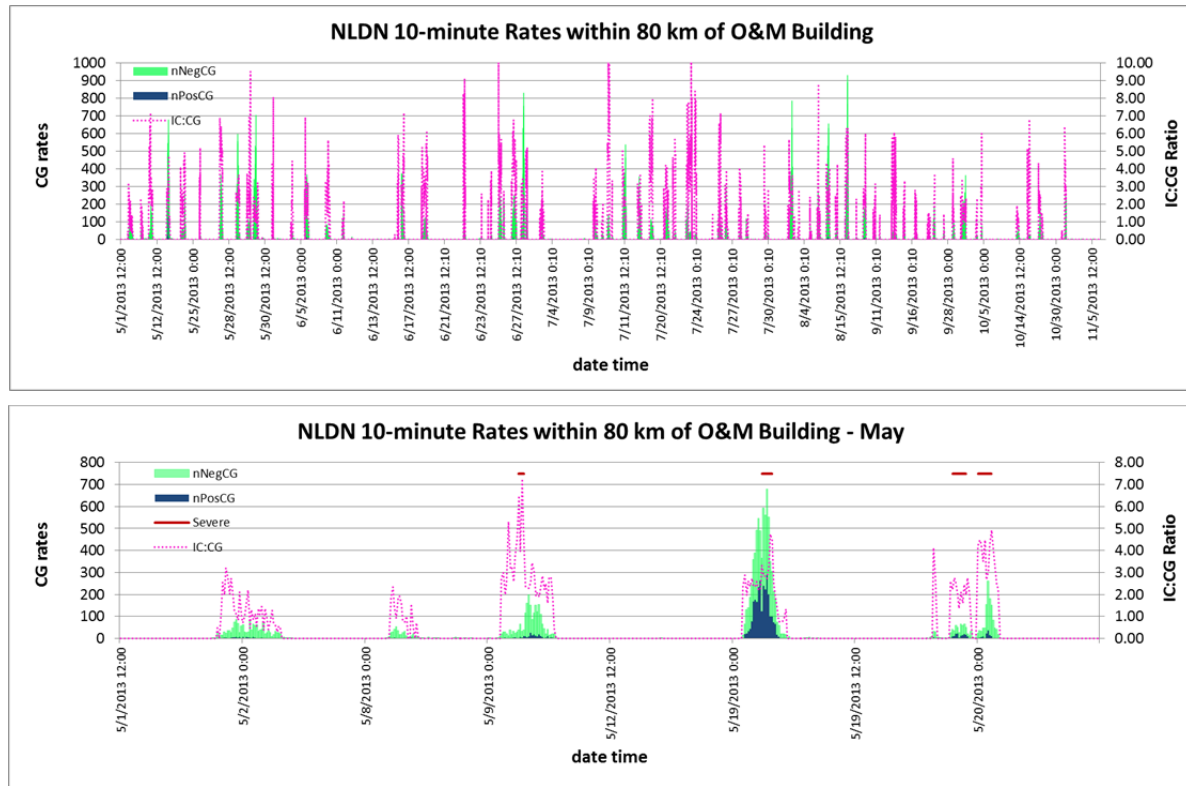
Fig. 7.　NLDN Lightning observations within 80 km of the O&M building, for 10-minue periods, including negative CG stroke count (green bars), positive CG stroke count (blue bars, not easily seen), and IC:CG ratio (cloud pulses / CG strokes). (a) Full season; (b) zoom-in of same display as (a) for the periods of May 1-20. Local severe storm report periods (large hail, tornados, and high surface winds) are indicated by red bars.
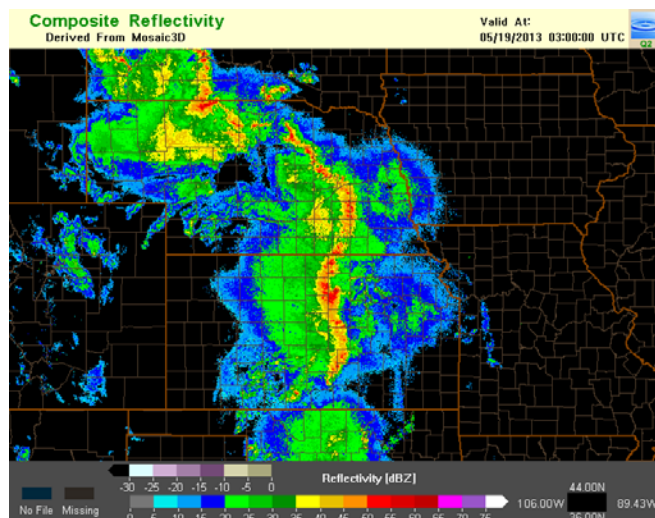

Fig. 8.　Composite reflectivity for inverted polarity storm on May 19 as it reaches the Kansas wind farm (traveling from west to east).
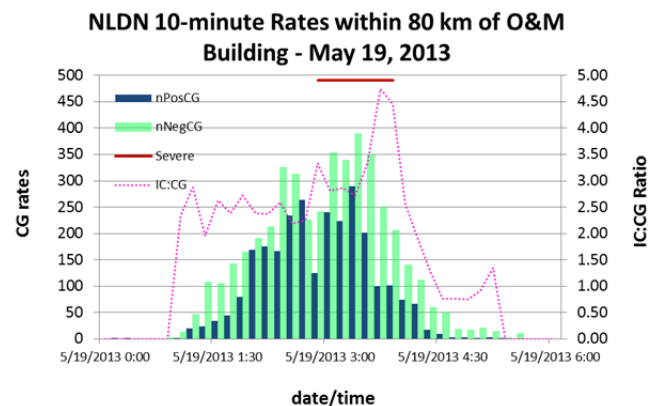

Fig. 9.　10-minutes counts and IC:CG ratio for the May 19 "inverted polarity" storm over the wind farm shown in Fig. 8.

Upon reaching the wind farm, the convective core of the storm produced hundreds of high-current positive CG flashes for each 10-minute period.   The NLDN reports in Fig. 9 suggest that about half of the ground discharges are positive. Actually, a closer look at the NLDN negative reports, evaluated in combination with the LMA data, suggest that most of them are negative polarity cloud pulses that exhibit waveforms similar to CG return strokes (Bill Rison, personal communication).   The impact of this storm on the wind farm is discussed in the following section.

Wind Turbine Interaction and Case Studies

During the 2013 campaign, there were 68 reports of lightning current in turbine blades produce by the SCADA system.   38 of these were judged to be single-turbine attachments produced by downward flashes, based on a combination of NLDN observations and experience derived from video observations of a subset of the flashes during 2012 and 2013. An additional 12 were likely upward flashes that were initiated by nearby positive CG flashes or horizontally-extensive cloud flashes. The remaining 18 SCADA reports were for simultaneous turbine blade attachments produced by upward and downward flashes. Based on our various video observations, we know that a number of upward flashes were not reported by the SCADA system, either because they did not produce any natural return-stroke-like events or because the events had very low peak currents. To our knowledge, all of the upward flashes were initiated from large storms, typically multicellular, that were decaying over the wind farm.

The May 19 inverted-polarity storm discussed above was particularly interesting. During an 11-minute period starting at 03:22z (when this storm was over the eastern portion of the wind farm) there were 16 SCADA reports produced by lightning attachment to turbine blades. All these reports were time-and space-correlated with NLDN events. Four of the NLDN events were associated with simultaneous SCADA reports from two turbines.   All NLDN reports were positive polarity CG strokes with peak current in the range of 53 to 191 kA. It is our intent to study this period in more detail in the future, including a detailed look at the charge-moment-change characteristic reported by the CMC Network.

We also note that FMA and Duke University maintained surveillance of the middle atmosphere above the wind farm using SpriteNet cameras located at Yucca Ridge, Bennett, CO and Lubbock, TX. Although no sprites were observed over the wind farm during the May 19 storm, several were observed during our field program. For the first time, a sprite was captured coincident with a video-captured upward flash, both of which were triggered by the same nearby +CG on 30 May 2013 (Lyons et al., 2014).

As noted above, there were several cases where the SCADA system reported "simultaneous" lightning-caused current transients in more than one turbine. One such case is discussed here, and is used as an example to illustrate many of the simultaneous observations at the wind farm.   During the nighttime hours of June 4, 2014 a large organized system with imbedded convection propagated from west to east across all of Kansas and northern Oklahoma. As the northern portion of this system approached the wind farm at around 07 GMT on June 5, it formed an east-west oriented line of small cells that weakened and stayed just south of the wind farm. However, the trailing stratiform region of the storm, with composite reflectivity values in the range of 35-45 dBZ, propagated directly over the wind farm between 08:40 UTC and 09:30 UTC. The composite reflectivity at 09:20z is shown in Fig. 10. Note the southwest-to-northeast orientation of the reflectivity boundaries, with a sharp east-west transition near the O&M building (magenta asterisk).

The flash rate near the wind farm was extremely low during this 40-minute period, with the NLDN reporting a total of 10 CG flashes within 20 km of the wind farm. Focusing on the 10-minute period starting at 09:20, there were four flashes reported by the LMA that had horizontally extensive channels within the wind farm. All four were associated with one or more NLDN reports. The LMA data for this 10-minute period is shown in Fig. 11. Fig. 11a shows the plan-view, with LMA sources color-coded by time. The location of the O&M building is depicted by the magenta asterisk. All four flashes originated in high-reflectivity regions (>55 dBZ) to the east and southeast of the wind farm, approached the wind farm from the east, and then traveled within the high-reflectivity stratiform region bisecting the wind farm. All flashes had horizontal extents greater than 60 km.

A time-height graph of LMA sources is provided in Fig. 11b, using the color scale shown in Fig. 11a. The time axis shows minutes and seconds. The four flashes that have channels within the wind farm perimeter are indicted by the circles at zero height. The open circles represent NLDN CG reports, and the black asterisks represent NLDN reports classified as cloud pulses. A careful review of LMA and NLDN waveform data for these four flashes indicates that the flash at 09:20:25 (left-most flash in Fig. 11b) was a cloud flash that was improperly classified by the NLDN. The other three flashes were also flashes with spatially extensive in-cloud channels, but they did include CG strokes.

The Mission Instruments EFM located 5.8 km southwest of the O&M building exhibited large field changes for all four of these flashes, as shown in Fig. 12. The EFMs measure potential gradient (right-hand vertical axis), so
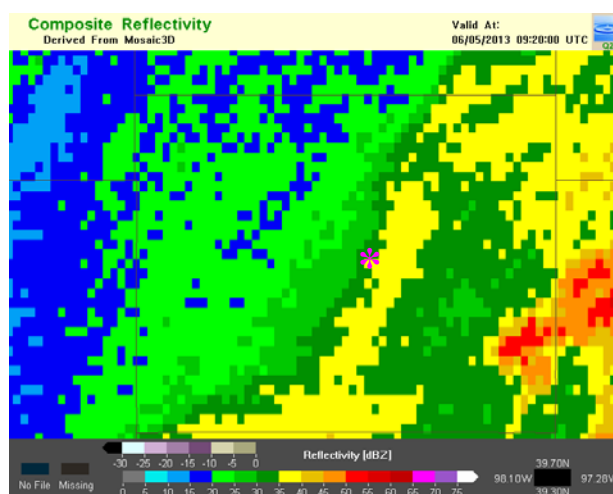

Fig. 10. Composite reflectivity showin trailing stratiform region on June 5 as it passes the Kansas wind farm (traveling from west to east). The O&M building (east-west center o fthe wind farm) is indicated by the magenta asterisk.
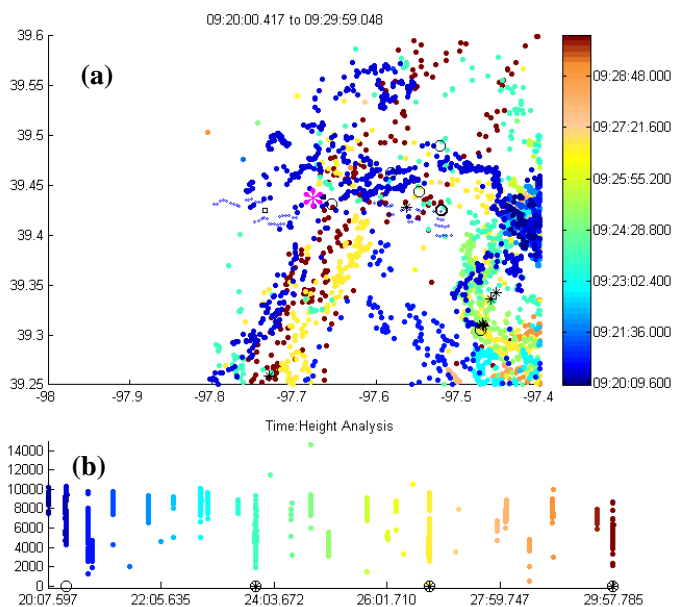

Fig. 11. LMA sources during a 10-minute period starting at 09:20 UTC on June 5. All sources are color coded by time. (a) plan view; wind turbines are small blue circles; NLDN reports are large black circles and asterisks; O&M building is the magenta asterisk. (b) time:height plot including LMA and NLDN reports. See text for details.

the polarity is the polarity of the dominant nearby charge aloft. At the beginning of this 10-minute period, the background field is about +3500 V/m, indicating "excess" positive charge aloft. NLDN CG reports are
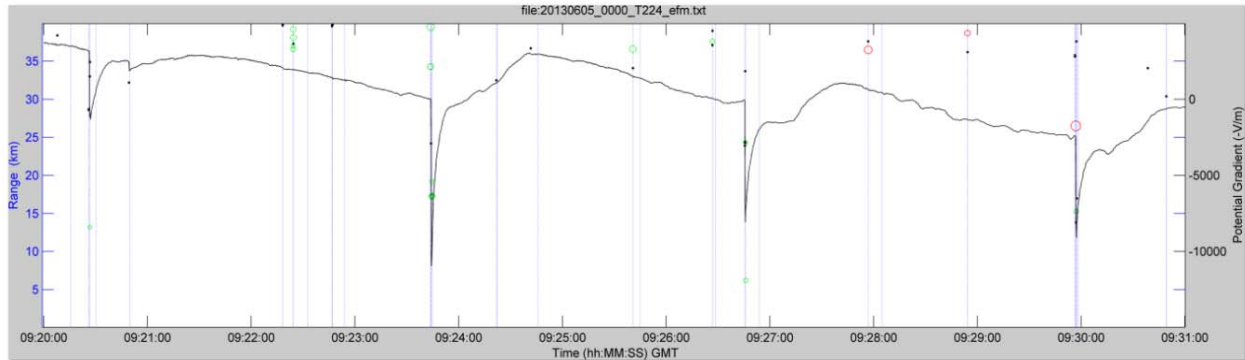

Fig. 12. West EFM recording for the time period of 09:20 to 09:30 om June 5, 2013. Four horizontall extensive flashes occurred over the wind farm during this period.   See text for details.

plotted in Fig. 12 as circles (red = positive; green = negative), with the diameter proportional to peak current. The vertical dotted lines indicate the times of all events within a specified range of the EFM (in this case 40 km). The black dots represent events classified by the NLDN as cloud pulses. The vertical displacement of the NLDN reports is proportional to the distance of the event from the west EFM in km, as indicated in left-had vertical axis. All four flashes removed positive charge from the stratiform region as they propagated over the wind farm, steadily reducing the local static field to about zero V/m by 09:31 UTC.

The flash that impacted two turbines began at 09:29:56.4 UTC. The LMA and NLDN data for this flash are shown in Fig. 13. The flash started in a convective core that was about 45 km southeast of the O&M building. The NLDN reported two cloud pulses at the time that the LMA sources transitioned from a height of about 4 km to 9 km, as shown in Fig. 13b. This flash propagated westward until it reached the high-reflectivity stratiform region shown in Fig. 10, at which time it turned to the northeast, and propagated within the stratiform region.

After propagating northeast for an additional ~20 km in about 150 ms ($\sim 1.3 \times 10^5$ m/s), the flash produced a 50 kA +CG stroke in the stratiform region near where it turned northeast, at 09:29:56.947. Immediately following this
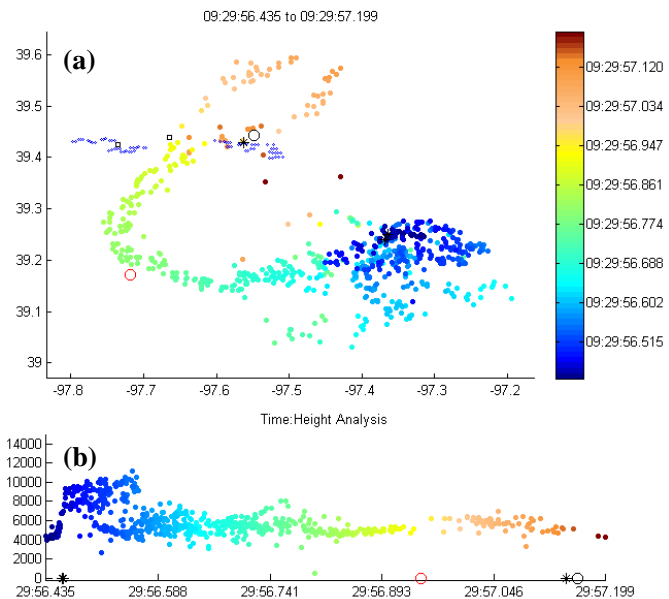

Fig. 13.   Cloud+CG flash starting at 09:29:56.4 UTC on June 5. This flash produced two positive CG strokes separated by 30 km., following by a negative CG stroke near the second positive stroke.

11

CG stroke, one of the two main horizontal channels turned eastward and traveled over a number of wind turbines. At 09:29:57.145. The NLDN reported an 81 kA positive event as cloud pulse (black asterisk) which was located within 210 m of the wind turbine that reported the highest current (of the two reporting turbines) on the SCADA system. A review of the magnetic field waveform data reported by the nearest NLDN sensor clearly shows that this event was a CG stroke. The (normal) waveform for the first (properly classified) +CG stroke is shown in Fig. 14a. The time axis in in µs and the amplitude is scaled in mV. For this NLDN sensor, one Volt is equivalent to radiation electric field strength of 26 V/m. The misclassified +CG stroke waveform is shown in Fig. 14b. The NLDN misclassified this event because of the existence of a bipolar second pulse that occurred within a few microseconds of initial peak. This second peak, with an amplitude of about half of the primary peak, is suggestive of a second nearby ground connection. Since the wind turbine with the

smaller SCADA-reported current was only 270 m from the first turbine, this waveform information supports the occurrence of near-simultaneous lightning currents in the two turbines.
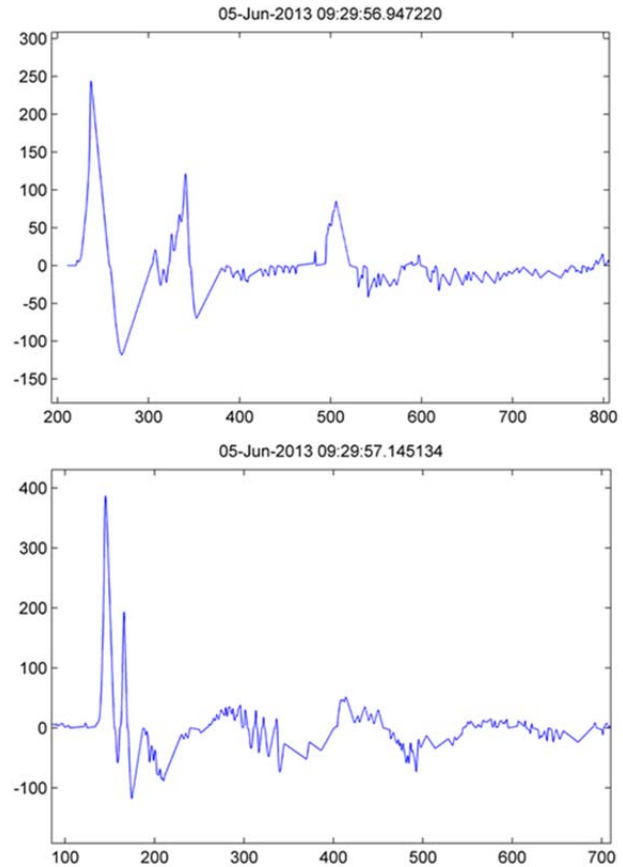

Fig. 14. Magnetic field waveforms for the two positive strokes associated with the flash shown in Fig. 13, recorded by the NLDN sensor nearest to the wind farm. (a) +50 kA CG stroke near windfarm; (b) +81 kA CG stroke that impacted two adjacent wind turbines.

Some portions of this particular flash were also caught on high-speed video, using a Miro 4 camera at 1000 fps. Four frames during the flash are shown in Fig. 15. Fig. 15a is the 1 ms frame that included the time of the first +CG stroke that was located south-southwest of the wind farm. This activity produce a large bright "blob" in the upper-right portion of the field-of-view. About 200 ms later, a number of framed depicted the downward propagating leader for the +CG stroke that impacted the two turbines. Fig. 15b shows one frame during the leader descent and Fig. 15c shows the last frame before saturation during the return stroke. The continuing current following the return stroke lasted for 94 ms. Fig. 15d is the first non-saturated field following the return stroke. Note that the leader channel is in exactly the same location as before the return strike (Fig. 15c), and shows no evidence of two separate channels near ground. The two yellow lines near the ground in Fig. 15d are the best estimates of the locations for the two turbines that reported current transients. The one on the right reported the highest current (16 kA), and the one on the left reported the lowest value that the SCADA system is capable of reporting (6 kA). As noted in Section II.D, these SCADA current values do not correlate well with NLDN estimated peak current, even when we had video evidence of direct attachment of a downward negative leader to the reporting turbine.

Based on these observations, it is likely that at most one of the turbines experience a direct strike – the one that was closest to the downward leader, closest to the NLDN location for the stroke, and reported the highest SCADA current value. It is reasonable to suspect that the other turbine initiated a short upward negative leader in response to the downward propagating positive leader just prior to the return stroke.
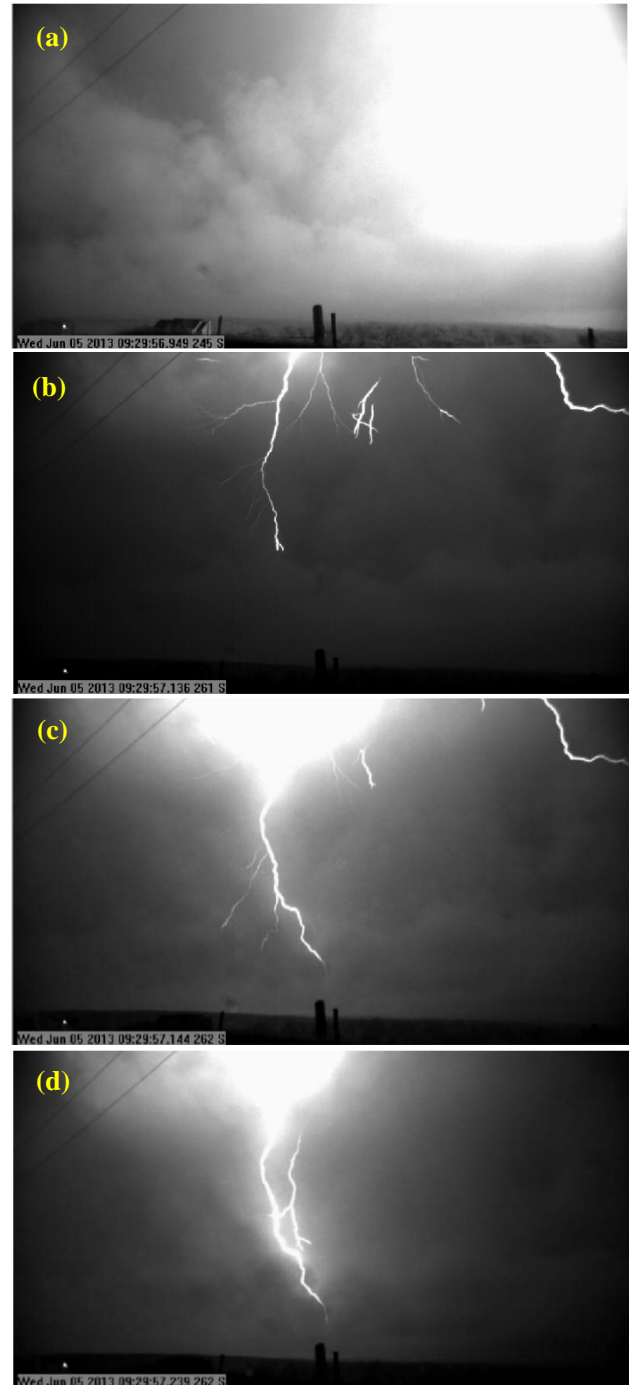

Fig. 15. Video frames from the 2-turbine flash on June 5, recorded by the Miro 4 camera recording at 1000 fps. (a) diffuse illumination from earlier +CG stroke ~50 km south-southwest of the camera location; (b) image of downward propagation positive leader about 8 ms before the +81 kA return stroke that struck the turbines; (c) just prior to +81 kA return stroke; (d) 95 ms after the return stroke. Yellow bars represent turbines that had SCADA reports.

Supporting details for this flash are provided by the nearby slow antenna records shown in Fig. 16. The top panel is for site "B", which is located near the west edge of the wind farm, remote from the path of this flash. The middle panel is for Site "C", which is east south-southeast of the wind farm, near the path of the first 1/3 of the flash as shown in Fig. 13. The lower panel is for site "D", located within 2 km of the two turbines that were impacted by the second +CG stroke. The times of the various NLDN reports are indicated just above the time axes, where red squares represent positive cloud pulses, red x's represent +CG strokes, green triangles represent -CG strokes, and green squares represent negative cloud pulses.

Fig. 16. Electric field waveforms from three of the eight slow antenna stations. See text for details.

The flash starts just before the time for the first reported cloud pulse just after 09:29:56.4 UTC. Very small positive electric field changes are observed by all sensors, due to their large distance to the flash initiation location. Field changes greater than 1 kV/m are seen by the Sites C and D after the 09:29:56.8 when the main channel of the flash turns north-northeast within the high-reflectivity stratiform region (see Figs. 10 and 13). The first +CG and its associated continuing current produces a large positive field change after 09:26:59.9, with a 7 kV/m change at Site D (closest site). Since Site D is within 2 km of the ground stroke location of the second +CG stroke (reported by the NLDN as a positive cloud pulse), its field is reversed during the approaching positive leader, and exhibits an abrupt 7 kV/m positive field change during the return stroke. Interestingly Site C, located near the southern portion of the flash extent but much farther from the ground strike location, sees as least as large of a positive field change during the return stroke (resulting in saturation), suggesting that significant positive charge aloft was removed near that site.

CLOSING COMMENTS

This paper provided an overview of the Kansas2012 and 2013 field programs that focused on obtaining detailed measurements of the behavior of lightning in and near a wind farm in Kansas. Ten groups collaborated on the 2013 field campaign, resulting in an immense dataset of complimentary observations. A summary of long-term lightning incidence in the area was provided, and compared with the conditions during the 2012 and 2013 campaigns. All instrumentation was briefly described. Two "cases" were used to highlight the observations – a positive-flash dominated storm that impacted 16 wind turbines in an 11-minute period, and an extensive flash that propagated more than 50 km and produced two widely-separated positive CG strokes, one of which impacted two wind turbines.

Analysis of these dataset are ongoing, providing validation information for Vaisala, practical insights for the wind farm owner, and scientific understanding to the community at large. Several initial analyses are reported at this meeting.
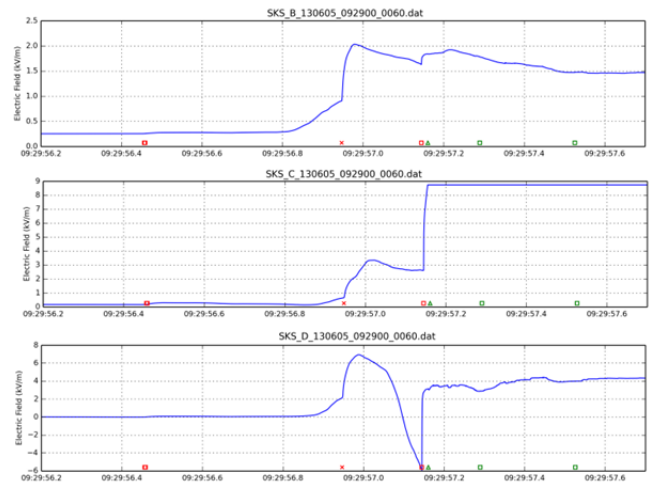
REFERENCES

Carey, L. D., and S. A. Rutledge, 2003: Characteristics of cloud-to-ground lightning in severe and nonsevere storms over the central United States from 1989–1998, J. Geophys. Res., 108(D15), 4483, doi:10.1029/2002JD002951.

Carey, L.D., Rutledge, S.A., Petersen,W.A., 2003; The relationship between severe storm reports and cloud-to-ground lightning polarity in the contiguous United States from 1989 to 1998. Mon.Wea. Rev., 131, 1211–1228.

Cummer, R.A. W.A. Lyons , M. A. Stanley, 2013; Three years of lightning impulse charge moment change measurements in the United States, J. Geophys. Res., 118, 5176-5189, doi:10.1002/jgrd.50442.

Cummins K.L., D. Zhang, M.G. Quick, A.C. Garolera, J. Myers, 2014: Performance of the U.S. NLDN during the Kansas Windfarm2012 and 2013 Field Programs, *23rd Intl. Lightning Det. Conf.*, Tucson, Arizona, USA, March 2014.

Fleenor, S. A., C. J, Biagi, K. L. Cummins, E. P. Krider, X.-M. Shao, 2009: Characteristics of Cloud-to-Ground Lightning in Warm-Season Thunderstorms in the Great Plains, Atmospheric Research, Vol. 91, pp 333-352, doi:10.1016/j.atmosres.2008.08.011.

Krehbiel, P. R.., R. J. Thomas, W. Rison, T. Hamlin, J. Harlin and M. Davis, 2000: GPS-based mapping system reveals lightning inside storms, Eos, Trans. Am. Geophys. Union, 81, 21.

Lyons, W.A., T.E. Nelson, T.A. Warner, A. Ballweber, R. Lueck, T.J. Lang, M.Saba, C. Schumann, S.A. Cummer, L. Zigoneanu, K. L. Cummins, M. Quick, W. Rison, P. Krehbiel, N. Beavis, S. Rutledge, J. Myers, T. Samaras, P. Samaras and C. Young, 2014: Meteorological aspects of two modes of lightning triggered upward lightning (LTUL) events in sprite-producing MCSs, *23rd Intl. Lightning Detection Conference,* Vaisala, Tucson, AZ.

Montanyà, J., van der Velse, O., E.R. Williams, 2014: Lightning Discharges Produced by Wind Turbines, J. Geophys. Res., doi: 10.1002/2013JD020225.

Murphy M.J., A. Nag, 2014: Enhanced cloud lightning performance of the U.S. National Lightning Detection Network™ following the 2013 upgrade, *23rd Intl. Lightning Det. Conf.*, Tucson, Arizona, USA, March 2014.

Rison, W., R. J. Thomas, P. R. Krehbiel, T. Hamlin and J. Harlin, 2000: GPS-based three-dimensional lightning mapping system: Initial observations in central New Mexico, Geophys. Res. Lett., 26, 3573.

Thomas, R. J., P. R. Krehbiel, W. Rison, S. J. Hunyady, W. P. Winn, T. Hamlin and J. Harlin, 2004: Accuracy of the Lightning Mapping Array, J. Geophys. Res., doi:10.1029/2004JD004549.

Warner, T., K.L. Cummins, R.E. Orville, 2012: Upward Lightning Observations in Rapid City, South Dakota and Comparison with National Lightning Detection Network Data, 2004-2010, J. Geophys. Res., v117, doi: 10.1029/2012JD018346.

Wilson, N., J. Myers, K.L. Cummins, M. Hutchinson, A. Nag, 2013: Lightning Attachment to Wind Turbines in Central Kansas: Video Observations, Correlation with the NLDN and In-Situ Peak Current Measurements, European Wind Energy Association Conference, Vienna, Austria, February 2013.